Sulfite-Activated Ferrate for Water Reuse Applications

Charles D. Spellman Jr.[a], Sahar Da'Er[b], Koaru Ikuma[b], Isabella Silverman[a], Joseph E. Goodwill[a*]

[a] *Department of Civil and Environmental Engineering, University of Rhode Island, Kingston, RI, 02881 USA*

[b] *Department of Civil, Construction and Environmental Engineering, Iowa State University, Ames, IA 50011 USA*

[*] *Corresponding Author*

Highlights

- Sulfite-Activated Ferrate is viable option for water reuse treatment
- Activation can lead to improved disinfection, pollutant oxidation, and fewer Br-DBPs
- Activation results in a stable colloidal suspension requiring coagulation
- Br-DBP formation risk exists, especially when activating super stoichiometrically
- Sub-stoichiometric FeSAOP is most effective and efficient, accentuating the role of Fe(IV)/Fe(V)

Abstract

Ferrate is a promising, emerging water treatment technology. However, there has been limited research on the application of Ferrate in a water reuse paradigm. Recent literature has shown that ferrate oxidation of target contaminants could be improved by "activation" with the addition of reductants or acid. This study examined the impact of sulfite-activated Ferrate in laboratory water matrix and spiked municipal wastewater effluents with the goal of transforming organic contaminants of concern (e.g., 1,4-dioxane) and inactivating pathogenic organisms. Additionally, the formation of brominated disinfection byproducts by activated ferrate were examined and a proposed reaction pathway for byproduct formation is presented. In particular,

the relative importance of reaction intermediates is discussed. This represents the first activated ferrate study to examine 1,4-dioxane transformation, disinfection, and brominated byproduct formation. Results presented show that the sub-stoichiometric ([Sulfite]:[Ferrate] = 0.5) activated ferrate treatment approach can oxidize recalcitrant contaminants by >50%, achieve >4-log inactivation of pathogens, and have relatively limited generation of brominated byproducts. However, stoichiometrically excessive ([Sulfite]:[Ferrate] = 4.0) activation showed decreased performance with decreased disinfection and increased risk of by-product formation. In general, our results indicate that sub-stoichiometric sulfite-activated ferrate seems a viable alternative technology for various modes of water reuse treatment.

Keywords: Activated ferrate; Water reuse; Advanced oxidation processes; Coagulation; Disinfection.

1. Introduction

Increasing demand for potable water has stressed water systems, accelerating the need for additional sources of water (Brown et al., 2013; Kummu et al., 2016). Secondary wastewater (MWW) effluent is a viable alternative water source (Asano and Levine, 1996; Huertas et al., 2008; Nichols, 1988). Reclaiming MWW, i.e., water reuse, can increase the capacity of water systems and decrease anthropogenic influence on surface waters (Anderson, 2003). However, water reuse also presents risks including associated with organic contaminants of emerging concern (CECs) and pathogenic organisms found in nearly all MWW effluents (Hendricks and Pool, 2012; Jelic et al., 2011; Kasprzyk-Hordern et al., 2009). Failure to remove CECs or inactivate pathogens during water reuse treatment can pose major health risks, regardless of end

use (Gennaccaro et al., 2003; Weber et al., 2006). Furthermore, the presence of effluent organic matter (EfOM), which can be detected even in effectively-treated MWW discharges (Shon et al., 2006), may result in downstream generation of disinfection by-products (DBPs) during reuse disinfection and oxidation processes. Water reuse systems must minimize these potential health risks to safely increase water supply.

As one of the largest global water reuse markets (Lassiter and Gleick, 2015), the state of California Department of Public Health has developed a framework to help mitigate risks from water reuse entitled Title 22 "Regulations Related to Recycled Water" (CA22). Many of the water reuse risks covered in CA22 can be addressed by adding strong oxidants, such as ozone (O_3), chlorine dioxide (ClO_2), or permanganate (MnO_4), to the treatment process. O_3 in particular is a widely deployed strong oxidant in water treatment, and has been shown to mitigate several risks associated with water reuse (Pisarenko et al., 2012). Although O_3 is generally effective, several disadvantages exist such as relatively complex equipment for onsite generation which challenges smaller municipalities that may benefit from water reuse (Daigger, 2009). Furthermore, oxidation with O_3 may result in compounds more toxic than target compounds (Dar et al., 2019), and may produce brominated DBPs if bromine (Br^-) is present in the system influent (Richardson et al., 1999; F. Wang et al., 2014). This is concerning for potential O_3-based (and other strong-oxidants) water reuse systems in water-scarce, coastal areas (e.g. southern and eastern Mediterranean, southwestern United States) where seawater intrusion leads to higher levels of Br^- in water systems (Barlow and Reichard, 2010; Demirel, 2004; Ged and Boyer, 2014).

High-valent iron species, specifically ferrate (Fe(VI)), are viewed as an alternative oxidant to O_3 and other strong oxidants (Jiang et al., 2019; Sharma et al., 2015; Yang et al.,

2013). Fe(VI) also offers associated operational advantages for water reuse systems including flexibility of being produced off-site by commercial Fe(VI) manufacturers as a stable salt (K_2FeO_4) (Monzyk et al., 2013), or generated on-site by an electrochemical method using commonplace water treatment chemicals (Ding et al., 2013; Jiang, 2014). Fe(VI) selectively oxidizes compounds generally considered CECs (Jiang, 2014; Sharma et al., 2016), inorganic contaminants (Goodwill et al., 2016; Virender K. Sharma, 2010), and inactivates pathogens (Daer et al., 2021; Hu et al., 2012; Schink and Waite, 1980). Fe(VI) can be "activated" yielding an advanced oxidation process (AOP) by addition of a reducing agent to generate an unknown combination of Fe(VI)-decay intermediates (i.e., "Fe(IV)/Fe(V)") and other radical species. The activation process enables greater transformation of recalcitrant CECs without increasing Fe(VI) dose (Sharma et al., 2021). Fe(VI) activation has been demonstrated via addition of various chemical reductants (e.g., thiosulfate), acids (e.g., HCl), UV light, silica gel, or carbon nanotubes (Ghosh et al., 2019; Manoli et al., 2018, 2017b, 2017a; Yang et al., 2021). Sulfite (SO_3^{2-}) has gained attention due to its relatively fast kinetics with Fe(VI) [$k = 10^{12}\ M^{-2}\ s^{-1}$] (Johnson and Bernard, 1992) and is proposed to activate Fe(VI) (i.e., "FeSAOP") in water treatment contexts due to high (>80%) transformation of CECs (Shao et al., 2019; Sun et al., 2018; Zhang et al., 2017). Some existing literature utilized sulfur-containing reductants for activation presumably due to broad acceptance of sulfite in wastewater treatment systems. The FeSAOP mechanism is believed to generate a combination of high-valent ephemeral iron intermediates (Fe(IV)/Fe(V)) plus certain radical species (e.g., SO_4^{-}•, •OH), likely as a function of [SO_3^{2-}]:[Fe(VI)] (Shao et al., 2020). As [SO_3^{2-}]:[Fe(VI)] increases, so does the amount of SO_4^{-}•/•OH formation relative to Fe(IV)/Fe(V). FeSAOP also changes the size distribution of resultant particles (Bzdyra et al., 2020), although this impact has been relatively under studied.

Even with prior research demonstrating promising Fe(VI)-based (i.e., activated and non-activated) oxidation and disinfection results, there is little research covering FeSAOP in water reuse applications relative to CA22 benchmarks. The overarching objective of this research was to demonstrate that sulfite-activated Fe(VI) (i.e., FeSAOP) can mitigate risks associated with pathogens and CECs, and serve as an appropriate option for water reuse systems. Specific aims were to: (1) assess oxidation performance on a relatively recalcitrant CEC specified by CA22, 1,4-Dioxane (14D), in varying water matrices; (2) quantify activation impacts on coagulation mechanisms; (3) evaluated some FeSAOP byproducts, specifically brominated byproducts (Br-DBPs), due to their higher associate health risks (Chu et al., 1982) and elevated formation potential in EfOM (Sirivedhin and Gray, 2005a); and (4) establish suitability as a disinfectant. These represent the novel contributions to advancement of FeSAOP in water reuse systems. Benchmarks for success were based upon the CA22 indirect potable reuse requirements.

2. Materials and methods

2.1. Chemicals and reagents

All chemicals and reagents used were commercially sourced and reagent grade. High purity (>92%), electrochemically generated potassium ferrate (K_2FeO_4) powder was obtained from Element 26 Technology (League City, TX), a commercial supplier of Fe(VI) (Monzyk et al., 2013, US Patent 8.449,756 B2). Reagent grade water (RGW) with resistivity of 18.2 MΩ.cm was generated by a Direct-Q 5 UV Milli-Q water system (MilliporeSigma; Burlington, MA).

114 2.2. Oxidation experiments

115 All experiments were performed in triplicate. 1L solutions were prepared of RGW with 5
116 μM 14D buffered at pH 8.0 (±0.1) with either 10mM phosphate or 10 mM tetraborate. Oxidation
117 experiments were performed in 2-L rectangular batch-reactors (PB-900 Programmable Jar
118 Tester, Phipps & Bird). The reactors were rapidly mixed (G ~ 150 s^{-1}) for 60 s, and dosed with
119 150 μM Fe(VI) from a stock solution. Rapid mixing time and intensity was minimized to balance
120 sample homogeneity and 14D volatilization (H_{14D} = 0.005 atm/(mol/L)). The 10mM Fe(VI)
121 stock solution, prepared immediately before each experiment, was buffered at pH 9.2 with 5mM
122 phosphate/0.3mM tetraborate with the Fe(VI) concentration confirmed spectrophotometrically at
123 510 nm (Rush et al., 1996). Each trial had a control (i.e., no Fe(VI)), Fe(VI)-alone, and an
124 FeSAOP reaction. The FeSAOP reactors were dosed with SO_3^{2-} 30 seconds after Fe(VI) had been
125 added. SO_3^{2-} was dosed in one sub-stoichiometric and one stoichiometrically excessive activation
126 ratio ([SO_3^{2-}]:[Fe(VI)]) of either 0.5 or 4.0, respectively, to demonstrate the impact of varying the
127 activation ratio. The [Fe(VI)] represents the molar Fe(VI) concentration at the time of activation
128 (30 s), not the initial Fe(VI) dose. The solutions were slow mixed (G ~ 50 s^{-1}) for 60 minutes
129 until Fe(VI) < 5 μM in each reactor, which was confirmed by the ABTS method (Lee et al.,
130 2005). Samples were passed through a 0.20 μm membrane filter (Whatman, Maidstone, U.K.)
131 placed into 20-mL headspace-free volatile organic analysis vials and stored at ~4 °C until
132 analysis. To simulate a water reuse scenario, experiments were repeated using two unchlorinated,
133 filtered (0.45μm, nylon membrane, Whatman) secondary MWW effluents in place of RGW.
134 Connecticut wastewater (CTWW) was collected at the Mattabassett District Water Pollution
135 Control Facility (Cromwell, CT) and Iowa wastewater (IAWW) was collected at the Ames Water
136 Pollution Control Facility (Ames, IA). Typical effluent water quality is given in Table SI-1. The

CTWW and IAWW samples were each buffered to pH 8.0 (±0.1) with 10mM tetraborate and contained 7.7 and 4.1 mg/L EfOM, respectively.

2.3. Brominated by-product generation

Solutions of RGW were buffered to pH 7.0 (±0.1) or 8.0 (±0.1) with 10mM tetraborate and contained dissolved (<0.45μm) organic carbon (DOC) concentrations of either 2.2 or 5.1 mg/L (Suwanee River natural organic matter (NOM), RO Distillate, IHSS). Solutions also contained 200 μM Br- intended to represent a worst-case scenario (similar to values tested by Huang et al., 2016 and Jiang et al., 2016). 250mL amber-glass jars (pre-washed with 10% acetone and rinsed with RGW) were filled with 200 mL of solution and sealed with threaded caps during experimentation. Experiments proceeded in the same manner explained in Section 2.2, having Fe(VI) dose of 150 μM and [SO_3^{2-}]:[Fe(VI)] of 0, 0.5 and 4.0, each tested in triplicate. Each reaction was allowed to run for 60 minutes, quenched with 2mM hydroxylamine, and then analyzed for Total THMs (i.e., chloroform, bromodichloromethane, dibromochloromethane, and bromoform) (TTHMs) immediately. TTHM experiments were repeated using the same CTWW and IAWW in place of RGW. Bromate was generated by dosing Fe(VI) at 150 μM with [SO_3^{2-}]:[Fe(VI)] of 0, 0.5 and 4.0 in solutions of RGW containing 200 μM Br- and buffered at pH 7.0 (±0.1) or 8.0 (±0.1) with 1mM tetraborate.

2.4. Analytical and statistical methods

14D analysis was performed using a gas-chromatograph (GC) with a mass-spectrometer detector (QP2010-SE, Shimadzu Corp.; Kyoto, Japan), following EPA 8270-E. The GC contained a 30-m Restek RxiR-624Sil column. Pre-filtered samples were injected and pre-

concentrated with a purge and trap (O-I-Analytical; College Station, TX) according to EPA method 5030-C and similar to those used by M. Sun et al. (2016). Quantification was performed by comparing 14D peak areas directly to the control samples (i.e., no oxidant added). Samples for non-purgeable organic carbon concentrations (DOC and EfOM) were quantified using a TOC-L (Shimadzu Corp.; Kyoto, Japan), calibrated with a potassium hydrogen phthalate standard per Standard Method 5030 (APHA, 2012). TTHMs were quantified using a GC with a surface acoustic wave (SAW) detector (THM-1000, Parker Hannifin Corp.; Huntsville, AL), following the approach of Ahmadi and Wu (2017). The THM instrument was externally calibrated with standards prepared from a 2,000 μg/mL THM-mix reference standard (Restek Corp.; Bellefonte, PA). Bromate was quantified by liquid chromatography-mass spectrometry (LCMS-8060, Shimadzu Corp.; Kyoto, Japan) equipped with an Aquasil C18 column. LCMS-8060 operating conditions followed a method optimized for this instrument in Shimadzu LCMS Application Note number C144 (Jiang et al., 2016; Tanaka and Horiike, 2017). Active bromine ($HOBr/OBr^-$) was determined using the Hach DPD Method 8016 (adapted from Standard Method 4500-Cl G, APHA, 2012). Values reported in figures represent the average of experimental replicates with error bars demonstrating two standard deviations (i.e., 95% confidence interval), unless noted otherwise.

2.5. Coagulation and flocculation of EfOM

Coagulation and flocculation processes used similar laboratory-prepared (5.1 mg/L DOC) and IAWW EfOM solutions at pH 7.0 as previously described in section 2.3. Pre-oxidation of EfOM by Fe(VI) and two activation ratios (similar to section 2.3) occurred in covered 600-mL glass beakers and mixed for 30 minutes. Resultant suspensions were then titrated with Nalcolyte

183 8100 (Nalco Water, Saint Paul, MN) cationic polyquaternary-amine-chloride polymer (specific
184 gravity = 1.16) until suspended particle negative surface charge had been titrated. Polymer was
185 diluted 1:200 immediately before coagulation experiments, and the volume of polymer solution
186 added was always <3% of total volume. Suspended particle surface charge was quantified *in situ*
187 *via* streaming current (Dentel et al., 1989) using a laboratory charge analyzer (Chemtrac LCA-
188 01, Norcross, GA). Once streaming current values were ~ 0, samples were allowed to flocculate
189 under gentle mixing ($G < 40\ s^{-1}$) for 30 minutes. Flocs were then counted using the light
190 obscuration method on a PC5000 particle counter (Chemtrac, Norcross, GA) using predefined
191 size-range channels. The range of countable particle diameters was between 2 and 125 μm.
192
193 2.6. *E. coli* disinfection and Fe(VI) activation
194 *Escherichia coli* K-12 cultures were grown in minimal media (MM) at room temperature
195 (22-23°C) with continuous orbital shaking at 160 rpm and allowed to reach late exponential
196 growth phase (optical density (OD) at 600nm = 0.5-0.6). MM details are described in Text SI-1.
197 Cells were harvested by centrifugation (8000 ×*g*, 2 min), washed twice using 10 mM tetraborate
198 buffer (pH 8.0±0.1), and subsequently resuspended in 10 mM tetraborate buffer (pH 8.0±0.1) or
199 MWW (CTWW or IAWW) for disinfection experiments. A 50 mM Fe(VI) stock solution was
200 prepared in 10 mM borate buffer (pH 9.0 ±0.1) prior to *E. coli* disinfection experiments and
201 utilized within 5 min of preparation to minimize Fe(VI) auto-decomposition. *E. coli* cell
202 suspensions were dosed with Fe(VI) and aliquots were subsequently withdrawn to quantify
203 Fe(VI) concentrations using the same ABTS method as previously mentioned. After 15 seconds
204 of Fe(VI) addition, cultures were dosed with SO_3^{2-} at [SO_3^{2-}]:[Fe(VI)] of 0, 0.2, 0.4, 0.8, and 3.0.
205 The time of SO_3^{2-} activation with respect to Fe(VI) addition was varied by introducing SO_3^{2-}

206 after 15, 30, 45 and 60 seconds of Fe(VI) addition. For all cell inactivation measurements, *E. coli*
207 cell concentrations were measured at 0 and 60 minutes of exposure by heterotrophic plate
208 counting following Standard Method 9215. Losses in culturable cells was considered inactivation
209 and calculated based on Equation SI-1.
210

211 **3. Results and discussion**

212 3.1. Dioxane Oxidation

213 Figure 1A presents the transformation of 14D by 150 μM Fe(VI) in two different buffers.
214 Results demonstrate limited transformation of 14D by Fe(VI) alone, with < 40% of 14D
215 oxidized. The phosphate-buffered sub-stoichiometric activation experiments yielded the most
216 significant ($p < 0.01$) improvement in transformation, increasing from 33% to 64%. Resultant
217 14D concentrations under these conditions approach the 0.5-log removal (69%) requirement set
218 under CA22. The transformation of 14D with increasing activation ratio showed no improvement
219 in borate and notably decreased performance in phosphate (< 20% transformation).

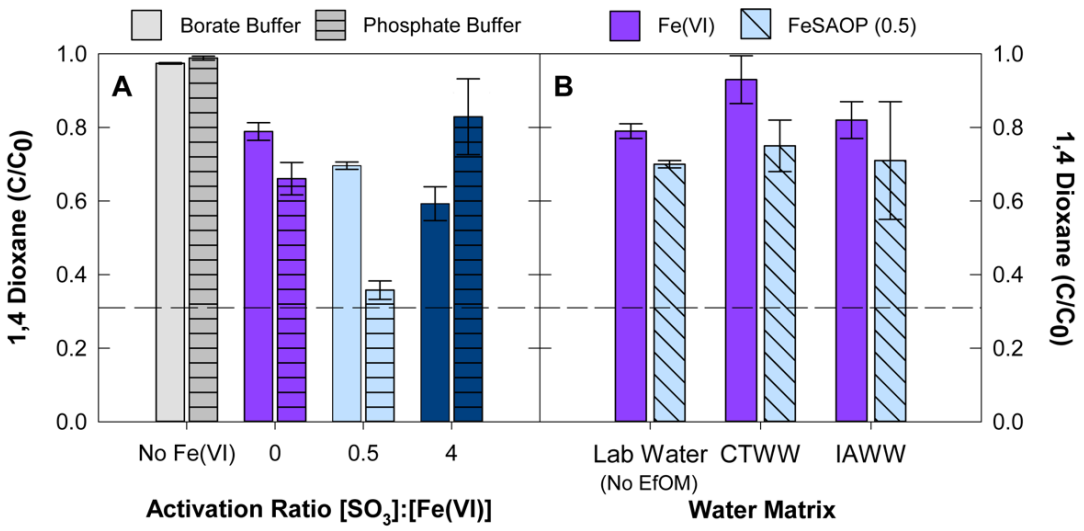

Figure 1: *(A) Transformation of 5 µM 14D by 150 µM Fe(VI) at pH 8.0 (±0.1) in 10mM Borate (solid bars) or 10 mM Phosphate (striped bars) buffer with increasing activation ratio. (B) Transformation of 5 µM 14D by Fe(VI) (solid bars) and FeSAOP (striped bars) in two MWWs, buffered with 10mM Borate at pH 8.0, and compared with RGW (no NOM) performance. FeSAOP [SO_3^{2-}]:[Fe(VI)] = 0.5:1. Dashed lines represents oxidation target set by CA22.*

The buffer significantly impacted 14D oxidation during activation. Huang et al. (2018) concluded borate-buffered Fe(VI) solutions yielded higher transformation of several CECs compared to phosphate buffered solutions due to nucleophilic complexation of Fe-species by phosphate ligands. However, this phenomenon noted by Huang et al. was not seen in our study where the 0.5 activation in phosphate yielded the highest oxidation, with only ~35% 14D remaining. In borate-buffered experiments both Fe(VI)-alone and 0.5-ctivation had significantly ($p < 0.02$) decreased oxidation performance compared to the same conditions with phosphate. Improved performance under 0.5 activation could imply 14D is more susceptible to oxidation by ephemeral iron species Fe(V)/Fe(IV) ($E^0 > 1.8$ V, Sharma, 2010) than SO_4^-•/•OH ($E^0 \approx 2.5$ V/2.7V, Giannakis et al., 2021) or Fe(VI) alone. The lower oxidation seen in borate buffers is

likely due to the formation of particulate Fe(III), which would have been sequestered in phosphate buffer, accelerating autocatalytic Fe(VI) decay in a way that does not lead to 14D transformation (Jiang et al., 2015). The decreased performance seen in stoichiometrically-excessive activation in phosphate buffer may be associated with the formation of phosphate radicals (e.g., HPO_4^{-}•) during activation. Both SO_4^{-}• and •OH react rapidly with buffer HPO_4^{2-} (k = 10^5 and 10^6 $M^{-1}s^{-1}$, respectively) to form HPO_4^{-}• (Mártire and Gonzalez, 2001; Maruthamuthu and Neta, 1978) and likely would only have occurred during 4.0 FeSAOP conditions. Phosphate radicals are shorter lived and generally 1-2 orders of magnitude less reactive with organics than SO_4^{-}• and •OH at circumneutral pH, implying a decreased oxidative performance (Bosio et al., 2005; Criado et al., 2012; Mártire and Gonzalez, 2001). However, the phosphate buffered experiments hold little practical implications for a water reuse scenario as the buffer phosphate concentration was two orders of magnitude higher than typical MWW influent phosphate concentrations (0.1-0.2mM, Metcalf & Eddy et al., 2013). For this reason, the use of a strong (10mM) phosphate buffer was not utilized in further experiments as the complete sequestration of resulting Fe(III) by phosphate does not offer an accurate representation of a typical water reuse matrix.

The impact on 14D oxidation due to MWW EfOM is presented in Figure 1B. Sub-stoichiometric activation showed no improvement in transformation in IAWW compared to Fe(VI) alone, but significantly improved ($p = 0.02$) oxidation by 18% in CTWW. Transformation was far from meeting CA22 0.5-log transformation goals in all conditions. Dosing Fe(VI) alone in CTWW was less effective compared to lab water, resulting in < 10% degradation, likely a result of the high EfOM (7.1 mg/L). These results imply that all oxidation conditions are impacted similarly by the presence EfOM and would not be appropriate for pre-oxidation of

259 certain recalcitrant MWW contaminants. These results agree with prior work suggesting the
260 effectiveness of SO_4^{-}•/•OH-based oxidation is impeded in the presence of EfOM, likely due to
261 sorption of target CECs to EfOM (Lian et al., 2017). However, similar impacts from EfOM were
262 also noted with O_3-based advanced oxidation processes (Pisarenko et al., 2012). Furthermore,
263 EfOM does not impact all contaminants equally. For example, oxidation of Mn(II) by Fe(VI)
264 was shown to be independent of NOM due to the Mn(II)-Fe(VI) reactions rapid kinetics
265 (Goodwill et al., 2016).

266 3.2. EfOM Coagulation

267 Figure 2A demonstrates the surface charge neutralization of laboratory Suwannee River
268 NOM and resultant iron particles by cationic polymer in RGW. NOM with no pre-oxidation
269 required 3.1 mg of polymer for complete negative charge titration, as indicated by the streaming
270 current results, while particles after pre-oxidation (all conditions) required greater than 4 mg of
271 polymer. The polymer required for complete titration varied only slightly (4.1-4.3 mg) between
272 the three methods of pre-oxidation. Polymer addition after pre-oxidation is in agreement with
273 prior studies where higher coagulant doses required after Fe(VI) pre-oxidation of NOM, due to
274 the cleaving of large molecules forming smaller hydrophilic molecules (Graham et al., 2010).
275 This phenomenon is not limited to Fe(VI) pre-oxidation, and has been noted with other pre-
276 oxidants (e.g., ozone) (Edwards et al., 1994; Schneider and Tobiason, 2000). However,
277 significantly higher (~1.5 to 3x) doses of polymer were required to obtain the point of zero
278 charge in MWW EfOM samples (Figure 2B). Converse to results in the lab water matrix, EfOM
279 absent of pre-oxidation demanded a higher polymer dose at 7.3 mg while the Fe(VI) pre-
280 oxidation required the lowest coagulant dose of 5.9 mg to achieve complete surface charge
281 neutralization. EfOM and Fe(VI) resultant particles after FeSAOP pre-oxidation were less

conducive to charge destabilization compared to Fe(VI) oxidation, similar to previously reported charge titrations (Bzdyra et al., 2020). Activation conditions each demanded nearly double the dose of polymer at 11.8 and 12.4 mg for $[SO_3^{2-}]$:[Fe(VI)] 0.5 and 4.0, respectively.

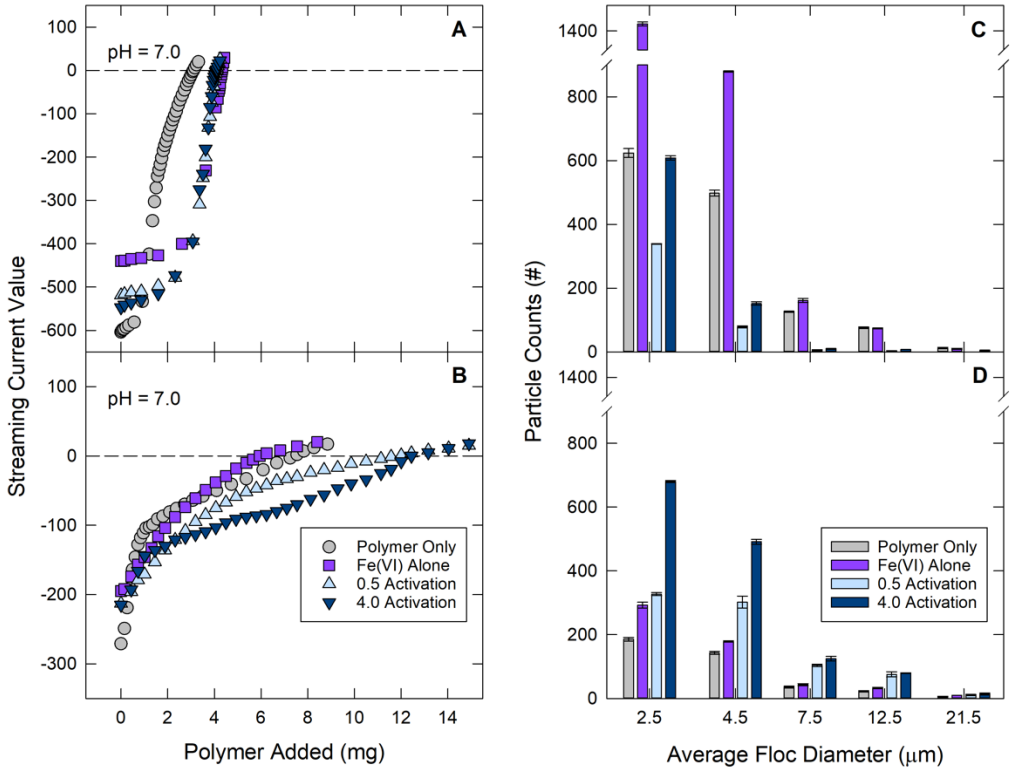

Figure 2: *Polymer mass required for particle destabilization of lab NOM (A) and EfOM (B) surface charge in 0.5 L of pH 7 suspensions using cationic polymer with and without pre-oxidation, and the resulting floc size after 30-min for lab NOM (C) and MWW sample (D).*

The polymer doses required for neutralization were similar to doses predictions based on the charge densities of the experimental solutions and the polymer. The charge density of the polymer was assumed to be 7.3 μeq/mg as previously reported for a quaternary polyamine polymer (Bolto and Gregory, 2007). The lab NOM solution was assumed to have an average charge density of 10.5 μeq/mg-DOC based on a previously determined value for Suwanee River NOM (Driver and Perdue, 2015) while the approximate average EfOM density was 25 μeq/mg

295 based on a previously reported range for EfOM of 19-31 μeq/mg (Cho et al., 2000). It was
296 estimated that the lab NOM and MWW, absent of Fe(VI), should require 3.5 and 7.1 mg doses of
297 polymer, respectively. The modeled estimates had good agreement with lab data, having an over
298 estimation by ~10% for lab NOM and only a 3% under estimation for EfOM. The required dose
299 was within 1.0 mg/L of the expected dose. The difference in polymer dose and rate of
300 destabilization between NOM and EfOM (< 5 mg vs > 8 mg polymer, respectively) is likely due
301 to the differing organic matter make ups. Surface water NOM generally contains a high fraction
302 of aromatic compounds (Mao and Schmidt-Rohr, 2004) while anthropogenically-influenced
303 EfOM typically contains more high-carbon aliphatic compounds along with a high fraction of
304 nitrogenated organics (Sirivedhin and Gray, 2005b). The aliphatic and nitrogenous compounds
305 increased the stability of Fe-particles in the EfOM suspension. The coating (i.e., adsorption) of
306 long aliphatic compounds unto Fe-oxides was demonstrated to alter particles electrostatic forces
307 resulting in re-stabilization of Fe-particles (Liang and Morgan, 1990), thus counteracting the
308 addition of polymer. Furthermore, organic nitrogen was shown to be less-emendable to Fe-based
309 coagulation mechanisms (Hu et al., 2016; Pietsch et al., 2001) and requires cationic polymer
310 dosing to destabilize particles complexed with organic nitrogen (Lee and Westerhoff, 2006). Our
311 results show both Fe(VI) alone and FeSAOP pre-oxidation resulted in stable colloidal
312 suspensions requiring further coagulation, regardless of organic matter type, to achieve
313 aggregation. However, all pre-oxidation methods used in a water reuse context (i.e., with EfOM)
314 required a higher polymer dose to achieve complete coagulation, likely due to the functional
315 nature of EfOM complexed with resultant particles.

316 The size of the resulting coagulated flocs are shown in Figure 2C and D. Generally, all
317 flocs formed had Z-average diameters < 5.5 μm under all conditions. All conditions were absent

of large-diameter (45-125 μm) NOM/EfOM particles before pre-oxidation and coagulation experiments. In RGW EfOM, Fe(VI) pre-oxidation produced the highest concentration of coagulated floc particles and the 0.5 activated resulted in the fewest. RGW EfOM flocs formed absent of Fe(VI) had the largest z-average diameter at 4.5 μm. Meanwhile both FeSAOP samples formed the smallest average floc size at 3.1-3.2 μm. These results are supported by prior work demonstrating FeSAOP results in a more polydisperse size distribution compared Fe(VI) (i.e., non-activated) particles, with FeSAOP particles smaller (and larger) than those generated by Fe(VI) (Bzdyra et al., 2020). These results differ from those obtained in MWW water trials. In MWW, the 4.0 activation resulted in the highest particle counts. The 0.5 activated resultant particles formed flocs with the largest z-average diameter (5.1 μm) while all other conditions resulted in flocs of similar, slightly smaller diameter (~4.5 μm). It is important to note that under all pre-oxidation conditions the resulting iron-based flocs (assuming $\rho = 1500$ kg/m^3, per Bache and Gregory, 2010) would have sufficient settling velocities (> 0.75 m/hr) to be removed via sedimentation within a recommended 4-hour settling time (10 State Standards). Remaining unsettleable small particles (d < 1.0 μm), likely in higher abundance under activation conditions (Bzdyra et al., 2020), would need to be removed via subsequent dual-media or membrane/ultra-filtration.

3.3. Disinfection performance

The results presented in Figure 3 show the $\log_{10}$ inactivation of *E. coli* by Fe(VI) and FeSAOP. Sub-stochiometric activation led to notable improvements (28%) to inactivation in buffered RGW, similar to improvements demonstrated in oxidation experiments (i.e., Figure 1). Enhancement in *E. coli* disinfection using FeSAOP is likely due to generation of Fe(V)/Fe(IV)

341 and SO_4^{-}•/•OH (Ghosh et al., 2006; Hu et al., 2012; Manoli et al., 2017a). Elevated inactivation
342 by FeSAOP may be due to limited gene expression (i.e., downregulation) during exposure which
343 differs from more conventional disinfectants (Daer et al., 2021). However, it is noteworthy that
344 stoichiometrically excessive FeSAOP significantly (p=0.0003) decreased *E. coli* inactivation by
345 75% compared to Fe(VI) alone, suggesting Fe(V)/Fe(IV) drive Fe(VI) disinfection. The
346 decreased inactivation may be a result of elevated cellular upregulation of oxidative-stress
347 response genes when exposed to SO_4^{-}•/•OH that is not seen when exposed to Fe(V)/Fe(IV) (Daer
348 et al., 2021) in addition to no contact time with ephemeral iron species. Kazama (1994) showed
349 that the addition of sodium thiosulfate with Fe(VI) led to a similar decrease in disinfection
350 capacity of Fe(VI) against F-specific RNA coliphage(Qβ), likely due to quenching of
351 disinfecting Fe(V)/Fe(IV) by the excess reductants. The average *E. coli* log inactivation by
352 Fe(VI) alone in IAWW and CTWW was 6.2±0.4 and 7.7±0.2, respectively, two orders of
353 magnitude higher than the average inactivation in RGW. These results are in agreement with
354 Manoli et al. where a 2-log improvement in murine norovirus inactivation by Fe(VI) was also
355 noted in MWW effluent compared to a lab matrix, possibly due to unintentional activation by
356 MWW constituents, such as NH_3, and subsequent formation of Fe(V)/Fe(IV) (Manoli et al.,
357 2020). Although still higher compared to RGW experiments, use of FeSAOP in IAWW and
358 CTWW resulted in a significant drop in *E. coli* inactivation by 20 and 11%, respectively (Figure
359 3). Results presented here are dissimilar to from 14D oxidation results, where FeSAOP had slight
360 improvements in MWW, but overall transformation was not better in MWW compared to RGW.
361 Some differences may have resulted from reaction kinetics. Although specific rates were not
362 determined in this study, inactivation of *E. coli*. by Fe(VI) is understood to be relatively fast (i.e.,
363 minutes, Gilbert et al., 1976), while oxidation of 14D by Fe(VI)-alone appears to be much slower

364 (e.g., < 20% transformation in RGW after 60 minutes, Figure 1) allowing for quenching by
365 EfOM. Although FeSAOP appears to be a viable option for disinfection in water reuse, further
366 examination, especially on role the Fe(VI)-derived intermediates during disinfection in MWW
367 matrices, is needed to identify active species and their involvement in the FeSAOP-specific
368 disinfection mechanism.
369

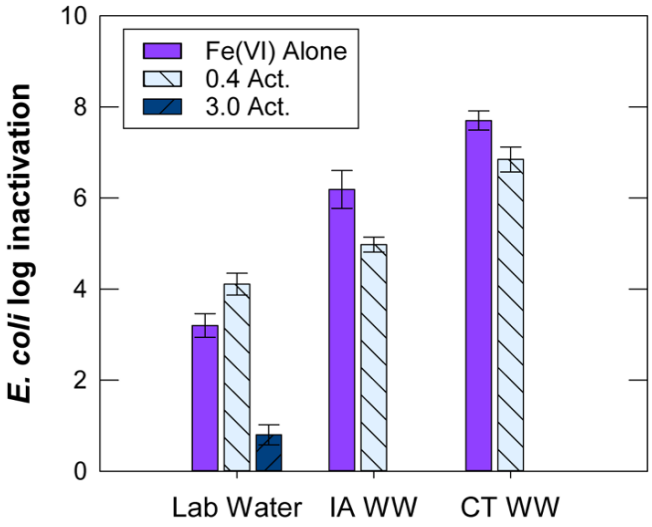

370

371 *Figure 3: E. coli inactivation buffered lab water and MWW at pH 8.0 (±0.1) at room temperature. Error*
372 *bars represent 1 standard error of at least three biological replicates. Initial cell concentration ~107*
373 *CFU/mL. 3.0 activation was not performed in MWW samples*

374 3.4. DBP Formation

375 The formation of select Br-DBPs were quantified under various Fe(VI) and FeSAOP
376 oxidation conditions. Figure 4 presents the generation of active bromine (i.e., HOBr/OBr-), a key
377 intermediate of Br-DBP formation, and bromate after Fe(VI) and FeSAOP oxidation. At neutral
378 pH, all oxidation methods produced similar concentrations of active bromine (~200 µg/L). While
379 activation may have been anticipated to generate more active bromine due to the presence of

Fe(V)/Fe(IV) and SO_4^-•/•OH, slightly faster production of H_2O_2 during FeSAOP (see Figure S1) likely suppressed active bromine formation (Jiang et al., 2016). 4.0 FeSAOP generated more than double the HOBr/OBr- compared to Fe(VI) alone and 0.5 activation when under more basic conditions (i.e., at pH 8). This observed difference at elevated pH is likely due to an order of magnitude increase in solution OH-, a precursor for •OH formation (e.g., OH- oxidation by SO_4^-• only under 4.0 FeSAOP, Shao et al., 2020). The increased •OH would have reacted with H_2O_2 more rapidly than HOBr/OBr- (10^7 vs 10^5 $M^{-1}s^{-1}$; Crittenden et al., 1999; Von Gunten and Oliveras, 1997) lowering the level of suppression and increasing HOBr/OBr- yields. The level of HOBr/OBr- formed suggests Br-DBP formation is an important consideration when treating elevated Br- waters with 4.0 FeSAOP. Furthermore, the formation of Br• during FeSAOP in Br-rich waters may also have impacts on the degradation of target contaminants (Dar et al., 2020).

All oxidation methods also produced BrO_3 (Figure 4B). Results show experimental conditions produced normalized BrO_3 yields (i.e., µg/L BrO_3/µM Fe(VI)) of 0.8 and 0.6 µg/L BrO_3/µM Fe(VI) at pH 7 and 8, respectively. Comparatively, prior work in borate buffer with the same $[Br-]_{initial}$ showed BrO_3/µM Fe(VI) of 0.9 and 1.5 at pH 6.2 and 7.5, respectively (Jiang et al., 2016). FeSAOP yielded less BrO_3 compared to Fe(VI) at pH 7.0, with 4.0 FeSAOP producing the lowest overall BrO_3 concentrations. BrO_3 yields by FeSAOP trended with pH, consistent with prior radical-based oxidation results where BrO_3 formation increased with pH (Guan et al., 2020; Pinkernell and Von Gunten, 2001). The opposite pH-effect was noted for Fe(VI)-alone where increased BrO_3 formation was observed with decreasing pH, which was also noted in prior studies (Huang et al., 2016; Jiang et al., 2016), likely resulting from the higher reduction potential associated with higher abundance of protonated Fe(VI) species (e.g., H_2FeO_4/$HFeO_4^-$) at relatively lower pH values (Sharma et al., 2016). Formation of elevated BrO_3

is explained by the HOBr/OBr- (a precursor to BrO_3) results previously presented, and due to the high $[Br-]_{initial}$ used in this study as BrO_3 formation by Fe(VI) oxidation generally increases proportionately with increasing $[Br-]_{initial}$ (Jiang et al., 2016). These results imply that reuse systems treating bromide-containing waters must use caution when implementing FeSAOP, as even with effective EfOM removal the formation of inorganic Br-DBPs remains. Decreasing pH in low-EfOM water may help decrease FeSAOP BrO_3 formation potential in water reuse systems. However, based on results from prior studies comparing Fe(VI) and O_3, yields from FeSAOP would likely be lower than BrO_3 resulting from O_3 under similar conditions (Jiang et al., 2019).

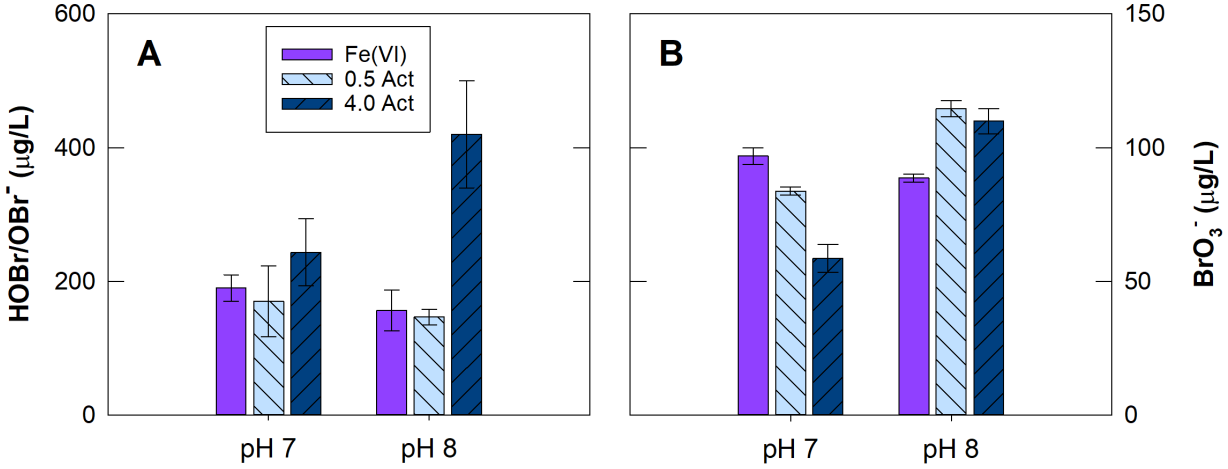

Figure 4: Generation of (A) active Bromine (HOBr/OBr-) in 10mM borate buffered RGW absent of NOM and (B) formation of Bromate in 1 mM borate buffer RGW absent of NOM.

The formation of bromoform in RGW with NOM is presented in Figure 5A&B. Under all conditions, bromoform concentrations were below the 80 µg/L Maximum Contaminant Level (MCL) for TTHMs set by CA22 and the U.S. Safe Drinking Water Act. However, chlorine was not present in the system elimination formation of chlorinated THMs. Fe(VI) alone formed < 20 µg/L of bromoform in every test condition. Prior work has shown Fe(VI) pre-oxidation generally

results in similarly low bromoform yields. Work by Huang et al. (2016) yielded only ~1 μg/L bromoform with notably different experimental conditions (e.g., 70% smaller Fe(VI) dose, an order of magnitude lower $[Br-]_{initial}$, etc.). FeSAOP sub-stoichiometrically at pH 7.0, bromoform yields were significantly ($p < 0.03$) lower when compared to Fe(VI) alone with changes of -39% and -32% in 2.2 and 5.1 mg/L NOM, respectively. This difference is also noted in Figure 4A (active bromine), and is likely a result of active oxidants shifting from Fe(VI) to primarily Fe(V)/Fe(IV) in the sub-stoichiometric FeSAOP mechanism (Shao et al., 2020). However, excess (i.e., 4.0) activation in lower NOM at pH 7 yielded more than double the bromoform concentration compared to Fe(VI) alone, and 3.5 times more than 0.5 activation. This is likely due to increased SO_4^{-}•/•OH generation by 4.0 FeSAOP compared to 0.5 FeSAOP (Shao et al., 2020) that preferentially result in bromoform formation in the presence of low molecular weight carboxylic acids (Y. Wang et al., 2014), which are relatively abundant in the NOM source used in this study (Palma et al., 2021). More than doubling the NOM increased the bromoform generation six-fold (10.7 to 61.4 μg/L) under 4.0 activation at pH 7 (e.g., Figure 5B). There was limited formation (< 6 μg/L) of bromoform at pH 8.0, independent of DOC concentration and activation ratio. Prior studies have shown that bromoform formation by Fe(VI) changes inversely proportional with pH (e.g., bromoform not detected at higher pH by Huang et al., 2016). This is most likely a result of the lower reduction potential of Fe(VI) at elevated pH due to the larger fraction of deprotonated Fe(VI) (e.g., FeO_4^{2-}), which generally reacts slower with target compounds (Jiang et al., 2016; Sharma, 2011). Only FeSAOP 4.0 activation in the

presence of 5 mg/L NOM had significantly different results ($p < 0.01$), with less bromoform resulting compared to Fe(VI).

Bromoform formation was also determined in unchlorinated Br-spiked MWW samples (Figure 5C). Experiments in both real MWW samples yielded less than 10 μg/L of TTHMs. Fe(VI) alone generated only 1.5 and 0.9 μg/L bromoform in CT and IAWW, respectively. These yields are similar (~1 μg/L) to those in aforementioned Fe(VI) studies (Huang et al., 2016). Activating at 0.5:1 produced negligible bromoform (< 1 μg/L) in either effluent. The higher activation ratio again yielded increased byproduct concentrations, showing 5-6 fold increased formation than Fe(VI) alone. This again is most likely due to shift in radical species during FeSAOP from Fe-based to SO_4^{-}•/•OH. Although the overall MWW yields were lower, the trend agrees with results in RGW matrix experiments. In general, these results suggest implementation of sub-stoichiometric FeSAOP at pH ≤ 7.0 would generate fewer Br-DBPs when compared to other tested oxidation methods and may be most viable conditions for water reuse applications. A proposed reaction pathway for formation of the measured Br-DBPs by FeSAOP radical pre-oxidation in a water reuse context is given in Figure 6. It is important to note that anything exhibiting oxidant demand (e.g., 14D) may alter these proposed reaction pathways and resulting yields of certain DBPs.

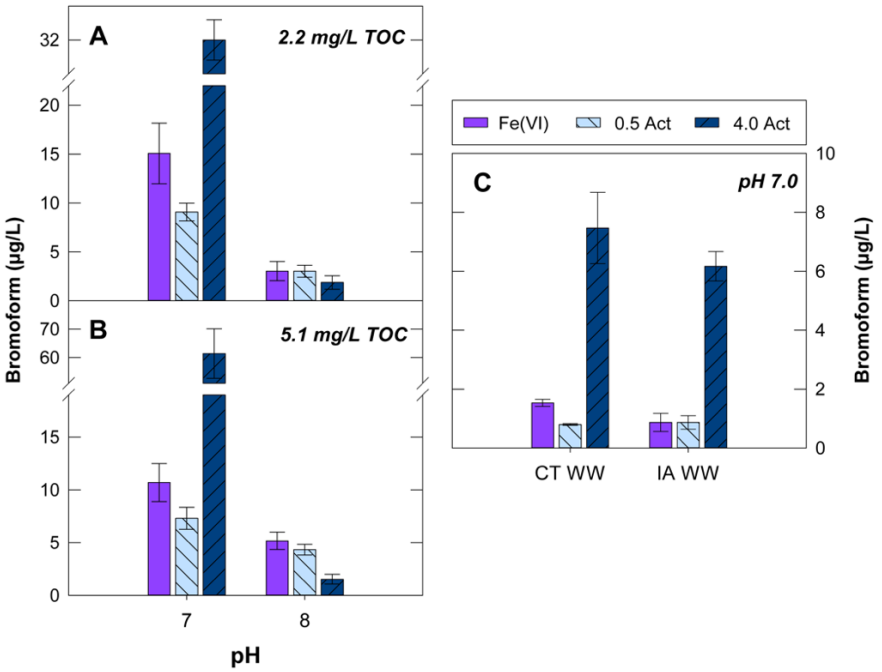

458

459 ***Figure 5:*** *Formation of Bromoform at pH 7.0 and 8.0 (10mM borate buffer) with 2.2 (A) and 5.1 (B)*

460 *mg/L of IHSS Suwannee River NOM. Bromoform was also quantified in pH 7.0 MWW (C). Other*

461 *measured THMs (chloroform, bromodichloromethane, dibromochloromethane) accounted for < 2 µg/L in*

462 *5C.*

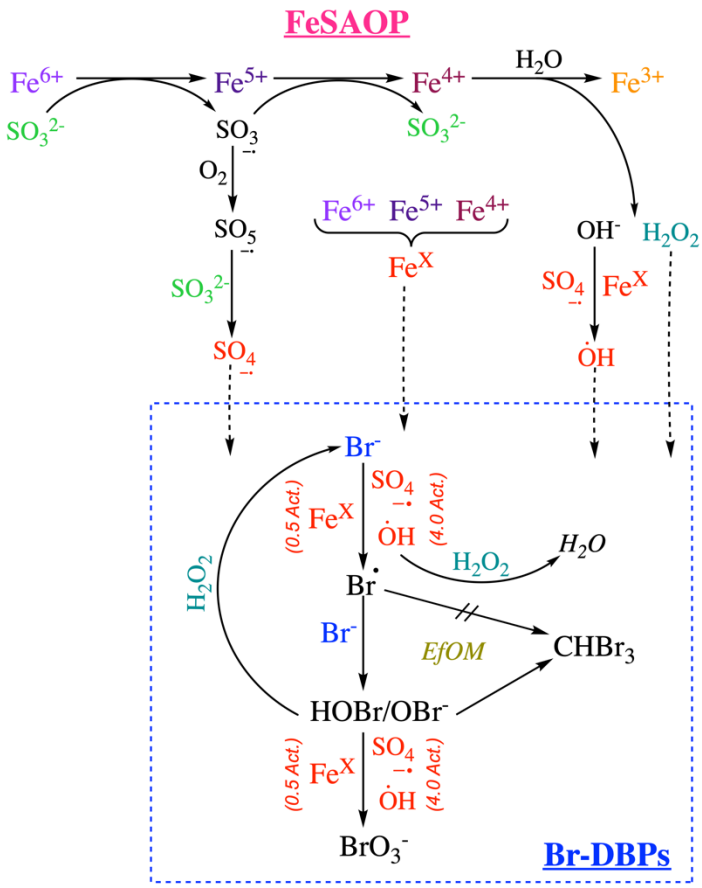

Figure 6: Proposed reaction mechanism for formation of measured Br-DBPs by FeSAOP in a water reuse paradigm

3.5. Implications For Water Reuse

FeSAOP as a water reuse technology that may address several aforementioned risks facing water reuse systems, including needs for inactivation of pathogenic organisms, destruction of residual suspended EfOM, and transformation of numerous CECs. Novel contributions from this study indicate that FeSAOP at [SO_3^{2-}]:[Fe(VI)] 0.5 could serve as a feasible alternative technology for some water reuse systems due to the combined mode of action (i.e., ephemeral iron species and radicals) leading to oxidation of recalcitrant CECs, inactivation of pathogens, and decreased direct Br-DBP formation. 0.5 FeSAOP was comparable to, or an improvement

474 over, Fe(VI)-alone in nearly all experimental trials. Although 4.0 FeSAOP may produce stronger
475 oxidative strength (due to SO_4^{-}•/•OH) resulting in oxidation of EfOM and certain CECs, it may
476 not be effective against all CECs (e.g., 14D) and does not inactivate pathogenic organisms. Also
477 stoichiometric-excessive activation leads to significantly elevated direct Br-DBP formation.
478 Reuse systems with elevated levels of Br^- in raw water should use caution when implementing
479 FeSAOP due to the potential risks of Br-DBPs. Furthermore, stoichiometric-excessive FeSAOP
480 simply acts as a mode for generation of SO_4^{-}• and •OH which several existing technologies also
481 accomplish (Giannakis et al., 2021; Miklos et al., 2018), while no existing technology provides
482 the combined mode of action with ephemeral iron species. Rural areas, often most impacted by
483 water scarcity, may especially benefit most from implementation of 0.5 FeSAOP due to certain
484 installation and operational simplicities compared to other technologies such as O_3 (Bauer, 2020)
485 and should be a point of focus in future research. Key remaining knowledge gaps include
486 operational proof of concept through pilot studies.
487

488 **4. Conclusions**

489 - 0.5 FeSAOP can improve oxidation of a recalcitrant organics compared to Fe(VI) alone
490 and may achieve CA22 benchmarks, but performance is highly dependent on water
491 quality and chemistry (e.g., buffer, EfOM, etc.).
492 - FeSAOP results in stable colloidal suspensions requiring subsequent coagulation to a
493 great extent than Fe(VI) alone, with FeSAOP requiring double the coagulant dose.
494 However, measured flocs from all oxidating conditions could be removed via
495 sedimentation.

- 0.5 FeSAOP leads to significantly less formation of measured Br-DBPs compared to 4.0 FeSAOP, likely through increased H_2O_2 formation resulting in suppression of HOBr/OBr^-.
- Sub-stoichiometric Fe(VI) activation results in adequate disinfection, however, inactivation is noticeably decreased at a $[SO_3^{2-}]$:[Fe(VI)] of 4.0, likely from instant quenching of all residual iron species leading to insufficient inactivation contact time.
- 0.5 FeSAOP may be the most advantageous option for water reuse systems, achieving improved transformation of contaminants and comparable disinfection performance to Fe(VI) while limiting direct formation of Br-DBPs.

5. Acknowledgments

Project funding provided by the U.S. Department of the Interior's Bureau of Reclamation (R17AC00133) and National Science Foundation CAREER Award (2046383). The expressed views are exclusively those of the authors, not the funding agencies The authors thank Element 26 Technology (400 Hobbs Road, Suite 107, League City, TX 77546; soundar.ramchandran@gmail.com; jtstrehl@gmail.com) for supplying the potassium ferrate product used in this work, and general collaboration. The authors thank undergraduate students Bradley Bzdyra, Ian Hallam, Jonathan Villada, and Michael Rothenbucher for laboratory contributions as well as Benjamin Cromwell and Dr. Thomas Boving for assisting the measurement of 1,4 dioxane.

6. References

Ahmadi, A., Wu, T., 2017. Inactivation of E. coli using a novel TiO 2 nanotube electrode. Environ. Sci.

Water Res. Technol. 3, 534–545. https://doi.org/10.1039/C6EW00319B

Anderson, J., 2003. The environmental benefits of water recycling and reuse. Water Sci. Technol. Water Supply 4, 1–10. https://doi.org/10.2166/ws.2003.0041

APHA, 2012. Standard Methods for Examination of Water and Wastewater (Standard Methods for the Examination of Water and Wastewater). Am. Public Heal. Assoc. Washington, DC, USA. https://doi.org/ISBN 9780875532356

Asano, T., Levine, A.D., 1996. Wastewater reclamation, recycling and reuse: past, present, and future. Water Sci. Technol. 33, 1–14. https://doi.org/10.1016/0273-1223(96)00401-5

Bache, D.H., Gregory, R., 2010. Flocs and separation processes in drinking water treatment: a review. J. Water Supply Res. Technol. 59, 16–30. https://doi.org/10.2166/aqua.2010.028

Barlow, P.M., Reichard, E.G., 2010. Saltwater intrusion in coastal regions of North America. Hydrogeol. J. 18, 247–260. https://doi.org/10.1007/s10040-009-0514-3

Bauer, S., 2020. Identification of water-reuse potentials to strengthen rural areas in water-scarce regions— the case study of Wuwei. Land 9. https://doi.org/10.3390/land9120492

Bolto, B., Gregory, J., 2007. Organic polyelectrolytes in water treatment. Water Res. 41, 2301–2324. https://doi.org/10.1016/j.watres.2007.03.012

Bosio, G., Criado, S., Massad, W., Rodríguez Nieto, F.J., Gonzalez, M.C., García, N.A., Mártire, D.O., 2005. Kinetics of the interaction of sulfate and hydrogen phosphate radicals with small peptides of glycine, alanine, tyrosine and tryptophan. Photochem. Photobiol. Sci. 4, 840–846. https://doi.org/10.1039/b507856c

Brown, T.C., Foti, R., Ramirez, J.A., 2013. Projected freshwater withdrawals in the United States under a changing climate. Water Resour. Res. 49, 1259–1276. https://doi.org/10.1002/wrcr.20076

Bzdyra, B.M., Spellman, C.D., Andreu, I., Goodwill, J.E., 2020. Sulfite activation changes character of ferrate resultant particles. Chem. Eng. J. 393, 124771. https://doi.org/10.1016/j.cej.2020.124771

Cho, J., Amy, G., Pellegrino, J., 2000. Membrane filtration of natural organic matter: comparison of flux decline, NOM rejection, and foulants during filtration with three UF membranes. Desalination 127,

283–298. https://doi.org/10.1016/S0011-9164(00)00017-5

Chu, I., Villeneuve, D.C., Secours, V.E., Becking, G.C., Valli, V.E., 1982. Toxicity of Trihalomethanes: I the Acute and Subacute Toxicity of Chloroform, Bromodichloromethane, Chlorodibromomethane and Bromoform in Rats. J. Environ. Sci. Heal. Part B 17, 205–224. https://doi.org/10.1080/03601238209372314

Criado, S., Rosso, J.A., Cobos, C.J., García, N.A., Mártire, D.O., 2012. Oxidation of ophthalmic drugs photopromoted by inorganic radicals. J. Photochem. Photobiol. A Chem. 244, 32–37. https://doi.org/10.1016/j.jphotochem.2012.06.018

Crittenden, J.C., Hu, S., Hand, D.W., Green, S.A., 1999. A kinetic model for H2O2/UV process in a completely mixed batch reactor. Water Res. 33, 2315–2328. https://doi.org/10.1016/S0043-1354(98)00448-5

Daer, S., Goodwill, J.E., Ikuma, K., 2021. Effect of ferrate and monochloramine disinfection on the physiological and transcriptomic response of Escherichia coli at late stationary phase. Water Res. 189, 116580. https://doi.org/10.1016/j.watres.2020.116580

Daigger, G.T., 2009. Evolving Urban Water and Residuals Management Paradigms: Water Reclamation and Reuse, Decentralization, and Resource Recovery. Water Environ. Res. 81, 908–823. https://doi.org/10.2175/193864708790893378

Dar, A.A., Chen, J., Shad, A., Pan, X., Yao, J., Bin-Jumah, M., Allam, A.A., Huo, Z., Zhu, F., Wang, Z., 2020. A combined experimental and computational study on the oxidative degradation of bromophenols by Fe(VI) and the formation of self-coupling products. Environ. Pollut. 258, 113678. https://doi.org/10.1016/J.ENVPOL.2019.113678

Dar, A.A., Wang, X., Wang, S., Ge, J., Shad, A., Ai, F., Wang, Z., 2019. Ozonation of pentabromophenol in aqueous basic medium: Kinetics, pathways, mechanism, dimerization and toxicity assessment. Chemosphere 220, 546–555. https://doi.org/10.1016/J.CHEMOSPHERE.2018.12.154

Demirel, Z., 2004. The history and evaluation of saltwater intrusion into a coastal aquifer in Mersin, Turkey. J. Environ. Manage. 70, 275–282. https://doi.org/10.1016/j.jenvman.2003.12.007

572 Dentel, S.K., Thomas, A. V, Kingery, K.M., 1989. Evaluation of the streaming current detector—I. Use
573 in jar tests. Water Res. 23, 413–421. https://doi.org/10.1016/0043-1354(89)90132-2
574 Ding, L., Li, X.Z., Lee, S.C., 2013. Kinetics of CH3S- reaction with in situ ferrate(VI) in aqueous alkaline
575 solution. Chemosphere 92, 1301–1306. https://doi.org/10.1016/j.chemosphere.2013.04.098
576 Driver, S.J., Perdue, E.M., 2015. Acid-base chemistry of natural organic matter, hydrophobic acids, and
577 transphilic acids from the Suwannee River, Georgia, as determined by direct potentiometric titration.
578 Environ. Eng. Sci. 32, 66–70. https://doi.org/10.1089/ees.2014.0356
579 Edwards, M., Benjamin, M.M., Tobiason, J.E., 1994. Effects of ozonation. On coagulation of NOM using
580 polymer alone and polymer/metal salt mixtures. J. / Am. Water Work. Assoc. 86, 105–116.
581 https://doi.org/10.1002/j.1551-8833.1994.tb06140.x
582 Ged, E.C., Boyer, T.H., 2014. Effect of seawater intrusion on formation of bromine-containing
583 trihalomethanes and haloacetic acids during chlorination. Desalination 345, 85–93.
584 https://doi.org/10.1016/j.desal.2014.04.021
585 Gennaccaro, A.L., McLaughlin, M.R., Quintero-Betancourt, W., Huffman, D.E., Rose, J.B., 2003.
586 Infectious Cryptosporidium parvum oocysts in final reclaimed effluent. Appl. Environ. Microbiol.
587 69, 4983–4984. https://doi.org/10.1128/AEM.69.8.4983-4984.2003
588 Ghosh, M., Manoli, K., Renaud, J.B., Sabourin, L., Nakhla, G., Sharma, V.K., Ray, A.K., 2019. Rapid
589 removal of acesulfame potassium by acid-activated ferrate(VI) under mild alkaline conditions.
590 Chemosphere 230, 416–423. https://doi.org/10.1016/j.chemosphere.2019.05.069
591 Ghosh, R.S., Dzombak, D.A., Luthy, R.G., Smith, J.R., 2006. In Situ Treatment of Cyanide-
592 Contaminated Groundwater by Iron Cyanide Precipitation. Water Environ. Res. 71, 1217–1228.
593 https://doi.org/10.2175/106143096x122456
594 Giannakis, S., Lin, K.Y.A., Ghanbari, F., 2021. A review of the recent advances on the treatment of
595 industrial wastewaters by Sulfate Radical-based Advanced Oxidation Processes (SR-AOPs). Chem.
596 Eng. J. 406, 127083. https://doi.org/10.1016/J.CEJ.2020.127083
597 Gilbert, M.B., Waite, T.D., Hare, C., 1976. Analytical Notes - an Investigation of the Applicability of

598 Ferrate Ion for Disinfection. J. / Am. Water Work. Assoc. 68, 495–497.
599 https://doi.org/10.1002/j.1551-8833.1976.tb02456.x
600 Goodwill, J.E., Mai, X., Jiang, Y., Reckhow, D.A., Tobiason, J.E., 2016. Oxidation of manganese(II) with
601 ferrate: Stoichiometry, kinetics, products and impact of organic carbon. Chemosphere 159, 457–464.
602 https://doi.org/10.1016/j.chemosphere.2016.06.014
603 Graham, N.J.D., Khoi, T.T., Jiang, J.-Q., 2010. Oxidation and coagulation of humic substances by
604 potassium ferrate. Water Sci. Technol. 62, 929–936. https://doi.org/10.2166/wst.2010.369
605 Guan, C., Jiang, J., Pang, S., Zhou, Y., Gao, Y., Li, J., Wang, Z., 2020. Formation and control of bromate
606 in sulfate radical-based oxidation processes for the treatment of waters containing bromide: A
607 critical review. Water Res. https://doi.org/10.1016/j.watres.2020.115725
608 Hendricks, R., Pool, E.J., 2012. The effectiveness of sewage treatment processes to remove faecal
609 pathogens and antibiotic residues. J. Environ. Sci. Heal. - Part A Toxic/Hazardous Subst. Environ.
610 Eng. 47, 289–297. https://doi.org/10.1080/10934529.2012.637432
611 Hu, H., Ding, L., Geng, J., Huang, H., Xu, K., Ren, H., 2016. Effect of coagulation on dissolved organic
612 nitrogen (DON) bioavailability in municipal wastewater effluents. J. Environ. Chem. Eng. 4, 2536–
613 2544. https://doi.org/10.1016/j.jece.2016.04.036
614 Hu, L., Page, M.A., Sigstam, T., Kohn, T., Mariñas, B.J., Strathmann, T.J., 2012. Inactivation of
615 bacteriophage MS2 with potassium ferrate(VI). Environ. Sci. Technol. 46, 12079–12087.
616 https://doi.org/10.1021/es3031962
617 Huang, X., Deng, Y., Liu, S., Song, Y., Li, N., Zhou, J., 2016. Formation of bromate during ferrate(VI)
618 oxidation of bromide in water. Chemosphere 155, 528–533.
619 https://doi.org/10.1016/j.chemosphere.2016.04.093
620 Huang, Z.-S., Wang, L., Liu, Y.-L., Jiang, J., Xue, M., Xu, C.-B., Zhen, Y.-F., Wang, Y.-C., Ma, J., 2018.
621 Impact of Phosphate on Ferrate Oxidation of Organic Compounds: An Underestimated Oxidant.
622 Environ. Sci. Technol. 52, acs.est.8b04655. https://doi.org/10.1021/acs.est.8b04655
623 Huertas, E., Salgot, M., Hollender, J., Weber, S., Dott, W., Khan, S., Schäfer, A., Messalem, R., Bis, B.,

Aharoni, A., Chikurel, H., 2008. Key objectives for water reuse concepts. Desalination 218, 120–131. https://doi.org/10.1016/j.desal.2006.09.032

Jelic, A., Gros, M., Ginebreda, A., Cespedes-Sánchez, R., Ventura, F., Petrovic, M., Barcelo, D., 2011. Occurrence, partition and removal of pharmaceuticals in sewage water and sludge during wastewater treatment. Water Res. 45, 1165–1176. https://doi.org/10.1016/j.watres.2010.11.010

Jiang, J.Q., 2014. Advances in the development and application of ferrate(VI) for water and wastewater treatment. J. Chem. Technol. Biotechnol. 89, 165–177. https://doi.org/10.1002/jctb.4214

Jiang, Y., Goodwill, J.E., Tobiason, J.E., Reckhow, D.A., 2019. Comparison of ferrate and ozone pre-oxidation on disinfection byproduct formation from chlorination and chloramination. Water Res. 156, 110–124. https://doi.org/10.1016/j.watres.2019.02.051

Jiang, Y., Goodwill, J.E., Tobiason, J.E., Reckhow, D.A., 2016. Bromide oxidation by ferrate(VI): The formation of active bromine and bromate. Water Res. 96, 188–197. https://doi.org/10.1016/j.watres.2016.03.065

Jiang, Y., Goodwill, J.E., Tobiason, J.E., Reckhow, D.A., 2015. Effect of Different Solutes, Natural Organic Matter, and Particulate Fe(III) on Ferrate(VI) Decomposition in Aqueous Solutions. Environ. Sci. Technol. 49, 2841–2848. https://doi.org/10.1021/es505516w

Johnson, M.D., Bernard, J., 1992. Kinetics and mechanism of the ferrate oxidation of sulfite and selenite in aqueous media. Inorg. Chem. 31, 5140–5142. https://doi.org/10.1021/ic00050a040

Kasprzyk-Hordern, B., Dinsdale, R.M., Guwy, A.J., 2009. The removal of pharmaceuticals, personal care products, endocrine disruptors and illicit drugs during wastewater treatment and its impact on the quality of receiving waters. Water Res. 43, 363–380. https://doi.org/10.1016/j.watres.2008.10.047

Kazama, F., 1994. Inactivation of coliphage Qβ by potassium ferrate. FEMS Microbiol. Lett. 118, 345–349. https://doi.org/10.1111/j.1574-6968.1994.tb06851.x

Kummu, M., Guillaume, J.H.A., De Moel, H., Eisner, S., Flörke, M., Porkka, M., Siebert, S., Veldkamp, T.I.E., Ward, P.J., 2016. The world's road to water scarcity: Shortage and stress in the 20th century and pathways towards sustainability. Sci. Rep. 6, 1–16. https://doi.org/10.1038/srep38495

Lassiter, A., Gleick, P., 2015. Sustainable Water: Challenges and Solutions from California, 1st ed. University of California Press.

Lee, W., Westerhoff, P., 2006. Dissolved organic nitrogen removal during water treatment by aluminum sulfate and cationic polymer coagulation. Water Res. 40, 3767–3774. https://doi.org/10.1016/j.watres.2006.08.008

Lee, Y., Yoon, J., von Gunten, U., 2005. Spectrophotometric determination of ferrate (Fe(VI)) in water by ABTS. Water Res. 39, 1946–1953.

Lian, L., Yao, B., Hou, S., Fang, J., Yan, S., Song, W., 2017. Kinetic Study of Hydroxyl and Sulfate Radical-Mediated Oxidation of Pharmaceuticals in Wastewater Effluents. Environ. Sci. Technol. 51, 2954–2962. https://doi.org/10.1021/acs.est.6b05536

Liang, L., Morgan, J.J., 1990. Coagulation of Iron Oxide Particles in the Presence of Organic Materials, in: Chemical Modeling of Aqueous Systems II. American Chemical Society, pp. 293–308. https://doi.org/10.1021/bk-1990-0416.ch023

Manoli, K., Maffettone, R., Sharma, V.K., Santoro, D., Ray, A.K., Passalacqua, K.D., Carnahan, K.E., Wobus, C.E., Sarathy, S., 2020. Inactivation of Murine Norovirus and Fecal Coliforms by Ferrate(VI) in Secondary Effluent Wastewater. Environ. Sci. Technol. 54, 1878–1888. https://doi.org/10.1021/acs.est.9b05489

Manoli, K., Morrison, L.M., Sumarah, M.W., Nakhla, G., Ray, A.K., Sharma, V.K., 2018. Pharmaceuticals and pesticides in secondary effluent wastewater: Identification and enhanced removal by acid-activated ferrate(VI). Water Res. 148, 272–280. https://doi.org/10.1016/j.watres.2018.10.056

Manoli, K., Nakhla, G., Feng, M., Sharma, V.K., Ray, A.K., 2017a. Silica gel-enhanced oxidation of caffeine by ferrate(VI). Chem. Eng. J. 330, 987–994. https://doi.org/10.1016/j.cej.2017.08.036

Manoli, K., Nakhla, G., Ray, A.K., Sharma, V.K., 2017b. Enhanced oxidative transformation of organic contaminants by activation of ferrate(VI): Possible involvement of FeV/FeIV species. Chem. Eng. J. 307, 513–517. https://doi.org/10.1016/j.cej.2016.08.109

Mao, J.-D., Schmidt-Rohr, K., 2004. Accurate Quantification of Aromaticity and Nonprotonated Aromatic Carbon Fraction in Natural Organic Matter by 13 C Solid-State Nuclear Magnetic Resonance. Environ. Sci. Technol. 38, 2680–2684. https://doi.org/10.1021/es034770x

Mártire, D.O., Gonzalez, M.C., 2001. Aqueous phase kinetic studies involving intermediates of environmental interest: Phosphate radicals and their reactions with substituted benzenes. Prog. React. Kinet. Mech. 26, 201–218. https://doi.org/10.3184/007967401103165253

Maruthamuthu, P., Neta, P., 1978. Phosphate radicals. Spectra, acid-base equilibria, and reactions with inorganic compounds. J. Phys. Chem. 82, 710–713. https://doi.org/10.1021/j100495a019

Metcalf & Eddy, I., Tchobanoglous, G., Stensel, H.D., Tsuchihashi, R., Burton, F., 2013. Wastewater Engineering: Treatment and Resource Recovery, 5th ed. McGraw-Hill Education, New York, NY.

Miklos, D.B., Remy, C., Jekel, M., Linden, K.G., Drewes, J.E., Hübner, U., 2018. Evaluation of advanced oxidation processes for water and wastewater treatment – A critical review. Water Res. 139, 118–131. https://doi.org/10.1016/J.WATRES.2018.03.042

Monzyk, I.B.F., Creek, T., Smeltz, A.D., Rose, J.K., 2013. Method for producing ferrate (V) and/or (VI). US 8.449,756 B2.

Nichols, A.B., 1988. Water Reuse Closes Water-Wastewater Loop. J. (Water Pollut. Control Fed. 60, 1930–1937.

Palma, D., Khaled, A., Sleiman, M., Voyard, G., Richard, C., 2021. Effect of UVC pre-irradiation on the Suwannee river Natural Organic Matter (SRNOM) photooxidant properties. Water Res. 202. https://doi.org/10.1016/j.watres.2021.117395

Pietsch, J., Sacher, F., Schmidt, W., Brauch, H.-J., 2001. Polar nitrogen compounds and their behaviour in the drinking water treatment process. Water Res. 35, 3537–3544. https://doi.org/10.1016/S0043-1354(01)00086-0

Pinkernell, U., Von Gunten, U., 2001. Bromate minimization during ozonation: Mechanistic considerations. Environ. Sci. Technol. 35, 2525–2531. https://doi.org/10.1021/es001502f

Pisarenko, A.N., Stanford, B.D., Yan, D., Gerrity, D., Snyder, S.A., 2012. Effects of ozone and

ozone/peroxide on trace organic contaminants and NDMA in drinking water and water reuse applications. Water Res. 46, 316–326. https://doi.org/10.1016/j.watres.2011.10.021

Richardson, S.D., Thruston, A.D., Caughran, T. V., Chen, P.H., Collette, T.W., Floyd, T.L., Schenck, K.M., Lykins, B.W., Sun, G.R., Majetich, G., 1999. Identification of new drinking water disinfection byproducts formed in the presence of bromide. Environ. Sci. Technol. 33, 3378–3383. https://doi.org/10.1021/es9900297

Rush, J.D., Zhao, Z., Bielski, B.H.J., 1996. Reaction of Ferrate (VI)/Ferrate (V) with Hydrogen Peroxide and Superoxide Anion - a Stopped-Flow and Premix Pulse Radiolysis Study. Free Radic. Res. 24, 187–198. https://doi.org/10.3109/10715769609088016

Schink, T., Waite, T.D., 1980. Inactivation of f2 virus with ferrate (VI). Water Res. 14, 1705–1717. https://doi.org/10.1016/0043-1354(80)90106-2

Schneider, O.D., Tobiason, J.E., 2000. Preozonation effects on coagulation. J. / Am. Water Work. Assoc. 92, 74–87. https://doi.org/10.1002/j.1551-8833.2000.tb09025.x

Shao, B., Dong, H., Feng, L., Qiao, J., Guan, X., 2020. Influence of [sulfite]/[Fe(VI)] molar ratio on the active oxidants generation in Fe(VI)/sulfite process. J. Hazard. Mater. 384, 121303. https://doi.org/10.1016/j.jhazmat.2019.121303

Shao, B., Dong, H., Sun, B., Guan, X., 2019. Role of Ferrate(IV) and Ferrate(V) in Activating Ferrate(VI) by Calcium Sulfite for Enhanced Oxidation of Organic Contaminants. Environ. Sci. Technol. 53, 894–902. https://doi.org/10.1021/acs.est.8b04990

Sharma, V.K., 2011. Oxidation of inorganic contaminants by ferrates (VI, V, and IV)–kinetics and mechanisms: A review. J. Environ. Manage. 92, 1051–1073. https://doi.org/10.1016/j.jenvman.2010.11.026

Sharma, Virender K., 2010. Oxidation of inorganic compounds by Ferrate (VI) and Ferrate(V): One-electron and two-electron transfer steps. Environ. Sci. Technol. 44, 5148–5152. https://doi.org/10.1021/es1005187

Sharma, Virender K, 2010. Oxidation of Inorganic Compounds by Ferrate(VI) and Ferrate(V): One-

Electron and Two-Electron Transfer Steps. Environ. Sci. Technol. 44, 5148–5152. https://doi.org/10.1021/es1005187

Sharma, V.K., Chen, L., Zboril, R., 2016. Review on High Valent FeVI(Ferrate): A Sustainable Green Oxidant in Organic Chemistry and Transformation of Pharmaceuticals. ACS Sustain. Chem. Eng. 4, 18–34. https://doi.org/10.1021/acssuschemeng.5b01202

Sharma, V.K., Feng, M., Dionysiou, D.D., Zhou, H.-C., Jinadatha, C., Manoli, K., Smith, M.F., Luque, R., Ma, X., Huang, C.-H., 2021. Reactive High-Valent Iron Intermediates in Enhancing Treatment of Water by Ferrate. Environ. Sci. Technol. https://doi.org/10.1021/acs.est.1c04616

Sharma, V.K., Zboril, R., Varma, R.S., 2015. Ferrates: Greener Oxidants with Multimodal Action in Water Treatment Technologies. Acc. Chem. Res. 48, 182–191. https://doi.org/10.1021/ar5004219

Shon, H.K., Vigneswaran, S., Snyder, S.A., 2006. Effluent Organic Matter (EfOM) in Wastewater: Constituents, Effects, and Treatment. Crit. Rev. Environ. Sci. Technol. 36, 327–374. https://doi.org/10.1080/10643380600580011

Sirivedhin, T., Gray, K.A., 2005a. 2. Comparison of the disinfection by-product formation potentials between a wastewater effluent and surface waters. Water Res. 39, 1025–1036. https://doi.org/10.1016/j.watres.2004.11.031

Sirivedhin, T., Gray, K.A., 2005b. Part I. Identifying anthropogenic markers in surface waters influenced by treated effluents: A tool in potable water reuse. Water Res. 39, 1154–1164. https://doi.org/10.1016/j.watres.2004.11.032

Sun, M., Lopez-Velandia, C., Knappe, D.R.U.U., 2016. Determination of 1,4-Dioxane in the Cape Fear River Watershed by Heated Purge-and-Trap Preconcentration and Gas Chromatography-Mass Spectrometry. Environ. Sci. Technol. 50, 2246–2254. https://doi.org/10.1021/acs.est.5b05875

Sun, S., Pang, S.Y., Jiang, J., Ma, J., Huang, Z., Zhang, J., Liu, Y., Xu, C.-B.C., Liu, Q., Yuan, Y., 2018. The combination of ferrate(VI) and sulfite as a novel advanced oxidation process for enhanced degradation of organic contaminants. Chem. Eng. J. 333, 11–19. https://doi.org/10.1016/j.cej.2017.09.082

Tanaka, M., Horiike, H., 2017. C144: Analysis of Bromate in Tap Water Using a Triple Quadrupole LC/MS/MS. Tokyo, Japan.

Von Gunten, U., Oliveras, Y., 1997. Kinetics of the reaction between hydrogen peroxide and hypobromous acid: Implication on water treatment and natural systems. Water Res. 31, 900–906. https://doi.org/10.1016/S0043-1354(96)00368-5

Wang, F., Ruan, M., Lin, H., Zhang, Y., Hong, H., Zhou, X., 2014. Effects of ozone pretreatment on the formation of disinfection by-products and its associated bromine substitution factors upon chlorination/chloramination of Tai Lake water. Sci. Total Environ. 475, 23–28. https://doi.org/10.1016/j.scitotenv.2013.12.094

Wang, Y., Le Roux, J., Zhang, T., Croué, J.P., 2014. Formation of brominated disinfection byproducts from natural organic matter isolates and model compounds in a sulfate radical-based oxidation process. Environ. Sci. Technol. 48, 14534–14542. https://doi.org/10.1021/es503255j

Weber, S., Khan, S., Hollender, J., 2006. Human risk assessment of organic contaminants in reclaimed wastewater used for irrigation. Desalination 187, 53–64. https://doi.org/10.1016/j.desal.2005.04.067

Yang, T., Mai, J., Cheng, H., Zhu, M., Wu, S., Tang, L., Liang, P., Jia, J., Ma, J., 2021. UVA-LED-Assisted Activation of the Ferrate(VI) Process for Enhanced Micropollutant Degradation: Important Role of Ferrate(IV) and Ferrate(V). Environ. Sci. Technol. acs.est.1c03725. https://doi.org/10.1021/ACS.EST.1C03725

Yang, X., Guo, W., Zhang, X., Chen, F., Ye, T., Liu, W., 2013. Formation of disinfection by-products after pre-oxidation with chlorine dioxide or ferrate. Water Res. 47, 5856–5864. https://doi.org/10.1016/j.watres.2013.07.010

Zhang, J., Zhu, L., Shi, Z., Gao, Y., 2017. Rapid removal of organic pollutants by activation sulfite with ferrate. Chemosphere 186, 576–579. https://doi.org/10.1016/j.chemosphere.2017.07.102

Supplementary Information

Sulfite activated Ferrate for Water Reuse Applications

Charles D. Spellman Jr.[a], Sahar Da'Er[b], Koaru Ikuma[b], Isabella Silverman[a], Joseph E. Goodwill[a*]
[a] *Department of Civil and Environmental Engineering, University of Rhode Island, Kingston, RI, 02881 USA*
[b] *Department of Civil, Construction and Environmental Engineering, Iowa State University, Ames, IA 50011 USA*

Number of pages: 2
Number of figures: 1
Number of tables: 1

Table SI-1: Typical MWW Effluent Water Quality obtained from facility records. N/A denotes value was not available in facility records at time of publication.

Parameter	**CTWW**	**IAWW**
Facility Name	Mattabassett District Water Pollution Control Facility	Ames Water Pollution Control facility
EPA Facility Look-up ID #	110001404178	110002039918
Flow ($x10^6$ gal/day)	24.4	10.1
pH	7.2	N/A
Biochemical Oxygen Demand (mg/L)	2.5	5.6
Total Suspended Solids (mg/L)	2.0	8.4
Nitrate (mg-N/L)	0.02	N/A
Total Phosphorus (mg/L)	0.77	4.7
Fecal Coliforms (#/100 mL)	2.7	N/A

Text SI-1: Additional Disinfection Methods

Bacteria media consisted of 0.3 g/L KH_2PO_4; 5.0 g/L K_2HPO_4; 0.5 g/L NaCl; 1.0 g/L $(NH_4)_2SO_4$; 0.12 g/L $MgSO_4.7H_2O$; 0.02 g/L $CaCl_2 \cdot 2H_2O$; 1.36 mg/L $FeSO_4 \cdot 7H_2O$; 0.24 mg/L $NaMoO_4 \cdot 2H_2O$; 0.10 mg/L $NiSO_4 \cdot 6H_2O$; 0.27 mg/L $ZnCl_2$; 14.6 mg/L EDTA (pH 8.0±0.1) supplemented with 1 g/L glucose from a 20% (w/v) stock glucose solution.

Log inactivation was calculated by:

[Eq. SI-1] $$\text{Inactivation} = \log_{10}\left(\frac{N_0}{N}\right)$$

where N_0 and N are E. coli cell concentrations (CFU/mL) present initially and following treatment, respectively.

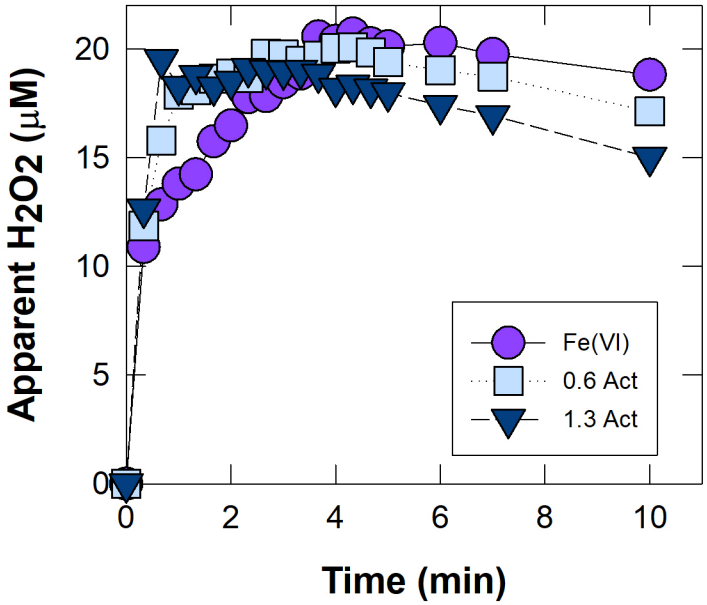

Figure S1: Apparent H_2O_2 formation over time after Fe(VI), 0.6, and 1.3 activation in pH 7.0 RGW, measured using the horseradish-peroxidase ABTS method, as described in Lee et al., 2014.

References

Lee, Y., Kissner, R., von Gunten, U., 2014. Reaction of Ferrate(VI) with ABTS and Self-Decay of Ferrate(VI): Kinetics and Mechanisms. Environ. Sci. Technol. 48, 5154–5162. https://doi.org/10.1021/es500804g